BIOCHEMISTRY
including biophysical chemistry & molecular biology

Current Topic

pubs.acs.org/biochemistry

Structural Basis for Activation of Voltage-Gated Cation Channels

Letícia Stock, Caio Souza, and Werner Treptow*

Laboratório de Biofísica Teórica e Computacional, Departamento de Biologia Celular, Universidade de Brasília, DF, Brasília, Brazil

ABSTRACT: Because of their remarkable roles in electrical cell signaling, voltage-gated cation channels (VGCCs) have been the subject of intense investigations and debate for more than 50 years. Ultimately, the prospective implications of such studies have an impact on our understanding of the molecular properties of VGCCs involved in consciousness, anesthesia, and diseases, to mention a few. The following review aims to summarize our current knowledge of activation of VGCCs by highlighting major methodological innovations in the field and the breakthroughs they allowed. Focusing mainly on insights gained through computer simulations, while acknowledging important experimental findings, we hope to inspire experimentalists to benefit from these approaches in the generation of hypotheses and design of experiments. Also, we outline major future challenges for the field, such as channel modulation, lesser-known receptors, and molecular origins of channel dysfunctions.

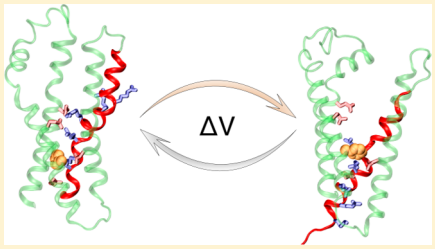

Voltage-gated cation channels (VGCCs) are membrane-embedded protein pores that assist the flow of selective ionic species across the cell membrane in response to a voltage stimulus. It is this property that defines these proteins as the fundamental molecular devices for diverse electrically mediated biological processes such as hormone regulation, cellular secretion, electric signaling in neurons, and contraction in excitable muscle cells.[1]

VGCCs make up a protein superfamily encompassing channels selective for Na^+, Ca^{2+}, and K^+, namely, Nav, Cav, and Kv, respectively, and those that discriminate only the cationic nature (HCN). Given their relevance in essential physiological processes, these channels are encoded by a substantial number of genes in higher organisms. Mutations in these channel genes are implicated in several human diseases, termed channelopathies.[2] Examples of channelopathies include hyperexcitability disorders and inheritable diseases such as epilepsy, cardiac long-QT syndrome, and neuromuscular diseases. The comprehension of the structure−function interplay of VGCCs promises the development of new approaches for the treatment of channelopathies, particularly by targeting malfunctioning channels.[3]

The following overview describes results obtained from a variety of VGCC structure−function studies, some of which trace back to early electrophysiology experiments, but centers on contributions from the computational modeling field. As such, this review is intended both to highlight successful methodological innovations in the field of ion channel molecular dynamics (MD) simulations and to inspire experimentalists to benefit from these theoretical approaches in the generation of hypotheses and design of experiments. Historically, a plethora of experimental data, including high-resolution X-ray structures and a large set of atomic-level information gathered from MD simulations, have been made available for Kv (*Shaker*) channels,[4,5] thereby making the K^+ channel the critical model for investigating the structural basis of activation in VGCCs. These structural studies of K^+ channels provide an invaluable resource for resolving future challenges in the field, namely the structural characterization of other members of the VGCC family, in light of the most recently determined X-ray structures of prokaryotic voltage-gated Na^+ channels.[6−9] Other appealing questions relate to the structural basis of inactivation in VGCCs, their modulation by ligands, including neurotoxins and anesthetics, and their channelopathies and related dysfunctions.

FUNCTIONAL STUDIES AND ACTIVATION MODELS OF VGCCS

Ingenious patch−clamp experiments[10] were critical in revealing the activation (opening) of VGCCs as the key voltage-dependent process by which the channel controls ionic conduction (Figure 1). At hyperpolarized potentials ($V < 0$), VGCCs are preferentially nonconductive resting (closed) structures. In response to membrane depolarization ($V > 0$), VGCCs switch on their active (open) state, exhibiting various levels of ionic conductance.[11] The molecular transition from the resting (closed) state to the active (open) state is known as the activation gating process of the channel. Although they are approximately 2 orders of magnitude smaller than ionic currents (G), the so-called "gating currents" were found to correspond to a fundamental observable of channel activation, given their strong voltage dependence and coupling to ionic currents. Since the pioneering work of Hodgkin and Huxley, gating currents and, more specifically, gating charges (Q), corresponding to the time integral of the gating current at a given voltage, have been measured for a variety of channels, as discussed extensively in refs 4 and 5. Typically, the activation process gives rise to a total Q of ∼12−14 e.[12−14]

Received: September 24, 2012
Revised: January 14, 2013
Published: January 14, 2013

   dx.doi.org/10.1021/bi3013017 | *Biochemistry* 2013, 52, 1501−1513

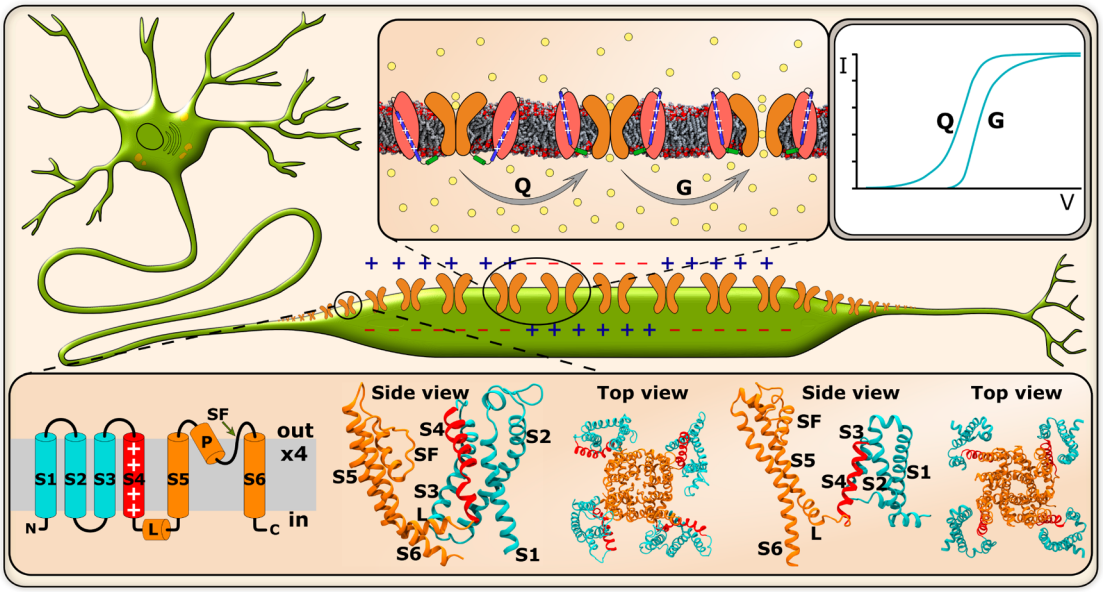

Figure 1. From macroscopic observables to atomistically detailed structures. Excitable cell, represented here by a neuron, with highlighted membrane-embedded VGCCs and their normalized measured gating (Q) and ionic (G) currents, which originated from reorganization of membrane-bound charged particles and flow of ions through the channel, respectively. From left to right, the bottom insets depict the VGCC topology, the channel subunit and tetrameric structure of Kv1.2 and those same structures of NavAb, respectively. Labels are S1−S6 for transmembrane helices, L for the linker, P for the pore helix, and SF for the selectivity filter.

As revealed by cloning and sequencing experiments[15,16] and also by recently determined X-ray crystallography structures (see below), VGCCs are either tetrameric or pseudotetrameric (Figure 1). The central pore forms from the arrangement of four transmembrane (TM) domains. Each subunit is composed of six TM helices, labeled S1−S6. Segments S5 and S6 constitute the central pore domain (PD) and delineate the pathway for the ionic current. A conserved motif between these segments forms the selectivity filter (SF), responsible for ion selectivity. Segments S1−S4, identified as the voltage sensor domain (VSD), connect to PD via an S4−S5 linker. In this helical bundle, S4 contains at least four highly conserved positively charged arginine amino acids, called hereafter R_1−R_4.

Experiments probing the contribution of the S4 basic residues to the total Q culminated in the identification of this charged helix as a critical element in channel activation.[4,5] Mutations of S4 charged residues have been shown not only to diminish the associated total Q but also to affect the voltage dependence of the channel. In these experiments, the contribution of the S4 basic residues was evaluated by neutralizing or reversing its positive charges and subsequently verifying the resulting Q, either directly or indirectly through the measurement of open pore probability.[14,17] The activation was envisioned to proceed via a complex mechanism involving VSD motions resulting essentially from S4 movements. Here, results from a plethora of experimental approaches, including the substituted cysteine accessibility method,[18,19] histidine scanning,[20] fluorescent labeling,[21] and second-site suppressor analysis and disulfide locking,[22−27] converged to show that S4 forms sequential state-dependent salt bridge interactions throughout its activation path, moving from a more internal binding site to a more external one.

Although agreeing to identify that S4 "senses" voltage variations triggering conformational changes that lead to channel activation, these early studies produced three putative activation mechanisms by which S4 could transfer Q across the low-dielectric membrane.[28] The first mechanism termed the sliding-helix or helical-screw activation model was originally proposed by Guy and Seerharamulu[29] and Catterall[30] and later adapted by other groups.[31,32] In the model, the S4 charged residues form sequential ion pairs with acidic residues on the neighboring S2 and S3 segments. Upon activation, the S4 helix goes through a large axial pistonlike motion (10−15 Å perpendicular to the membrane plane) crossing a focused, motionless electric field, while rotating ∼180° to the left. In contrast, the mechanism described by the transporter model of Bezanilla proposes that hydration of S4 focuses the electric field within the VSD and activation involves reshaping this intensely focused field around S4 rather than extensively displacing the segment across the membrane.[33−35] Under modifications of the local dielectric environment of S4, a relatively small TM movement of the S4 charges, accompanied by a rotation and a possible helical tilt, would suffice to account for the total gating charges.

In 2003, following the publication of the crystallographic structure of a Kv channel from the archaeon *Aeropyum pernix*, KvAP,[36] another model for the activation of VGCCs was proposed. This model states that S4 and the C-terminal region of S3, designated S3b, form a "voltage-sensor paddle" that neighbors the intracellular surface when the channel is closed. Upon activation, this paddle would move a large distance of ∼20 Å within the membrane. However, the model was refuted by many years of contradicting evidence, and it has now been admitted that the channel may have been crystallized in a non-native conformation. A revised version of the paddle model, based on the X-ray crystal of the "paddle chimera" Kv1.2−Kv2.1 channel,[37] proposes that the paddle moves ∼15 Å relative to helices S1 and S2, rather than tilting to a horizontal position. Moreover, a concertina-like transition of S4 from α- to 3_{10}-helix as it passes through the narrowest region of the VSD is thought to prevent S4 charges from being exposed to the lipid membrane, discarding the need for helix twist.

dx.doi.org/10.1021/bi3013017 | *Biochemistry* 2013, 52, 1501−1513

ACTIVATION OF VGCCS: INSIGHTS FROM MD STUDIES OF KV CHANNELS

For many years, an improved understanding of VGCC structure and function was hindered by the scarcity of atomic-level structural and dynamical data. This limitation is due primarily to the difficulty of obtaining atomistic structural data, by either X-ray diffraction, electron microscopy, or nuclear magnetic resonance (NMR). As evidence, it was only in 2005 that the first and only crystallographic structure of a mammalian voltage-gated K^+ channel, the Kv1.2 channel, was resolved (Figure 1).[38] The latter, pertaining to the *Shaker* family, was crystallized in the open activated state, allowing researchers to begin to answer essential questions about VGCCs. At large, the structure reveals a TM-oriented VSD only loosely attached to the pore, and in opposition to previous hypotheses, S4 is not shielded from the membrane by a protein canal but rather faces helices S1−S3 on one side and a lipid surface on another. Furthermore, the structure depicts the S4−S5 linker as a short α-helical segment lying at the inner membrane−water interface where, via its atomic contacts with the S6-crossing helical bundle, the segment bridges S4 to the main gate region of the channel. The same overall structural patterns have also been found in the recently determined X-ray structure of the Kv1.2−Kv2.1 paddle chimera.[37]

With the release of the Kv1.2 crystal structure, a number of efforts employing MD simulations and related methodologies were performed to characterize activation of the new channel. As described below, the accuracy with which force fields were able to reproduce a channel's properties, such as conduction, gating motions, and modulation by ligands, is a clear testament to the competence of the approach in the study of such complex molecular systems.[39]

Molecular Dynamics Simulations. The principle of MD simulations consists simply of generating a trajectory for a finite set of particles through multiple-time step numerical integration of classical equations of motion.[40] The final goal of computing a MD trajectory is to estimate any thermodynamic property $\langle A \rangle$ of an ergodic system in the form of a temporal average $\overline{A}_t$, i.e., $\lim_{t\to\infty} \overline{A}_t = \langle A \rangle$. The potential energy $U(r^N)$, characteristic of an N-particle system, in which r^N corresponds to the set of N atomic Cartesian coordinates, is the main function in MD. $U(r^N)$ associated with molecular parameters, obtained via quantum mechanics and experiments, corresponds to the so-called force field that accounts for bonded and nonbonded interactions in the system. In successful approaches,[41−45] the force field treats these interactions as a single effective potential, which can be written as

$$U(r^N) = \sum_{\text{bond}} k_r(r - r_0)^2 + \sum_{\text{angle}} k_\theta(\theta - \theta_0)^2 + \sum_{\text{dihedral}} \sum_{n} \frac{U_n}{2}[1 + \cos(n\varphi - \gamma)] + \sum_{\substack{i<j \\ (i,j)>1-4}} \varepsilon_{ij}\left[\left(\frac{R_{ij}^*}{r_{ij}}\right)^{12} - 2\left(\frac{R_{ij}^*}{r_{ij}}\right)^{6}\right] + \sum_{\substack{i<j \\ (i,j)>1-4}} \frac{q_i q_j}{4\pi\varepsilon r_{ij}} \quad (1)$$

where k_r and r_0 correspond to bond strength and chemical equilibrium position, respectively; k_θ and θ_0 are the angle force constant and its equilibrium value, respectively; $^1/_2U_n$, n, and γ are the torsional barrier, its frequency and its phase, respectively;q_i is the partial electric charge of atom i; ε is the dielectric constant; and, finally, R_{ij}^* and ε_{ij} match the parameters and van der Waals forces for the atomic pairs $\{ij\}$, respectively. In eq 1, bonded interactions are explicitly described by bond, angle, and dihedral terms.

Briefly, in the method, integration of Newton's equations is accomplished for every atom i with an infinitesimal time step δt on the order of 2 fs. Different schemes for controlling temperature and pressure can be applied to sample an *NPT* ensemble, as a way of simulating experimental conditions. An infinitesimal δt is required to ensure energy E conservation throughout the simulation and comes with the expense of a substantial computational time. As such, MD simulations are usually conducted with open source codes[46,47] that scale to hundreds of processors on high-end parallel platforms for systems of any size, making it feasible to complete continuous calculations in a short time. At present, it is possible to perform hundreds of nanosecond time scale MD simulations for >200000-atom systems. Nonetheless, a special purpose machine, named "Anton", capable of simulating equally large systems on the millisecond time scale,[48] has been recently designed, expanding the range of issues potentially tackled by MD simulations.

MD Simulations of the Membrane-Bound Activated Structure of Kv1.2. One of the first contributions of MD applied to the study of Kv1.2 activation has derived from simulations intended for the investigation of the structure of the open activated state of the channel embedded in the membrane (Figure 2).[49,50] In these studies, the simulation setup consisted of Kv1.2 embedded in a fully hydrated phospholipid bilayer. The protein was simulated either with or without the N-terminal tetramerization (T1) domain, to simplify the study system.[51] In these simulations, the VSD was described as an hourglass-like structure in which water penetrates from the extra- and intracellular sides exposing S4 charges to the solvent, consistent with the earlier accessibility and histidine scanning measurements. MD simulations of the VSD alone[52] in the membrane and NMR experiments further corroborated these results.[53] Specific salt bridge interactions between S4 arginines and neighboring VSD acidic residues and membrane−lipid heads were shown to stabilize the domain conformation.[49,50] In detail, R_1−R_4 are exposed to the externally accessible extracellular milieu, forming salt bridges with the following binding sites: PO_4^- outer membrane layer lipid headgroup and E^{183}, E^{226}, and E^{236}, respectively; the residues are located in segments S1, S2, and S2, respectively (Figure 3, top).

Electrostatic Calculations of Kv1.2 Embedded in the Membrane. The exquisite electric sensitivity of Kv1.2 relies on a number of intrinsic electrostatic properties related to the transport of gating charges during activation. In the context of MD simulations, investigation of such properties has relied primarily on the accurate computation of the electrostatic potential arising from the channel charges, ions, and dielectric properties of the environment. The initial efforts to electrostatically describe Kv1.2 and related channels[54] considered a continuum mean-field approximation based on the Poisson−Boltzmann (PB) equation, which assumes that the distribution of charges in the system is related to the electrostatic potential according to Boltzmann statistics

dx.doi.org/10.1021/bi3013017 | *Biochemistry* 2013, 52, 1501−1513

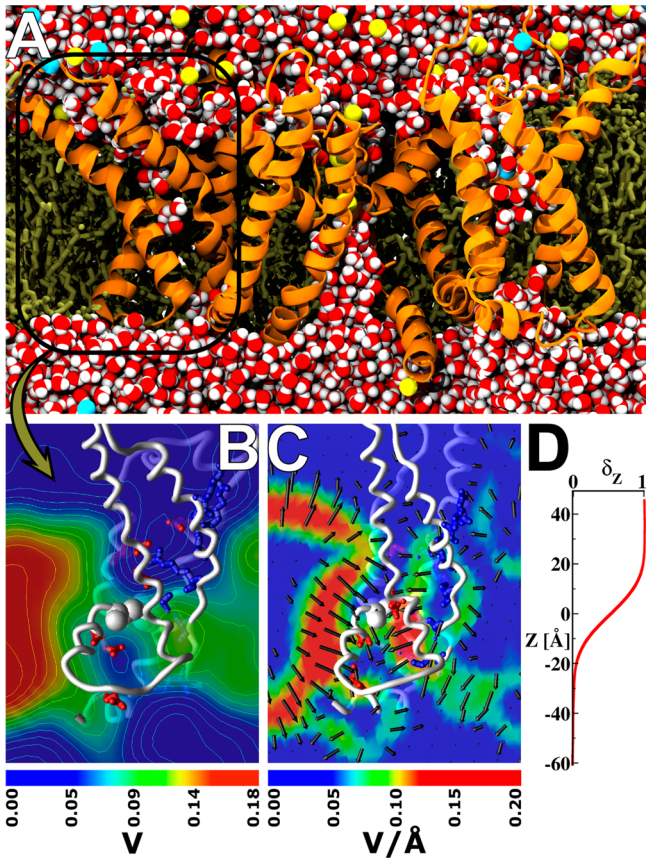

Figure 2. Structural details and electrostatic properties of Kv1.2 embedded in the membrane. (A) Typical atomistic MD simulation system of Kv1.2 embedded in a fully hydrated phospholipid bilayer. The system contains the channel (orange) with two K^+ ions (yellow) in the selectivity filter, 390 lipid molecules (ochre), 36280 solvent water (red) molecules, and salt in solution (a total of ~150000 atoms). A black frame highlights the VSD and its hydration structure. (B) Two-dimensional electrostatic potential map depicting the VSD environment when no TM potential is applied to the system. Note that the aqueous (blue) environment of the gating charges (blue licorice) and acidic residues (red licorice) carried by the VSD (white ribbons) collapses the electrostatic potential around F^{233} (white spheres). (C) Two-dimensional map of the electric field within the activated VSD structure under a hyperpolarized TM potential. (D) Electrical distance profile (δ_Z) through the VSD as a function of Z, the normal to the bilayer.

$$\nabla\cdot[\varepsilon(r)\nabla\Phi(r)] - \bar{k}^2(r)\Phi(r) = -4\pi\rho(r) \quad (2)$$

where $\Phi(r)$ is the electrostatic potential, $\rho(r)$ is the fixed charge density, and $\varepsilon(r)$ and $\bar{k}(r)$ are the position-dependent dielectric and ionic screening constants, respectively. Later, three-dimensional electrostatic potential (EP) maps for the Kv1.2–membrane system were determined independently by taking into consideration an MD-generated ensemble of equilibrium configurations of the channel,[49] in which every point charge of the system was explicitly considered to solve Poisson's equation

$$\nabla^2\Phi(r) = -4\pi\sum_i \rho_i(r) \quad (3)$$

where $\Phi(r)$ and $\rho_i(r)$ are the electrostatic potential and the charge density at r, respectively. In practice, the point charge can be approximated by a spherical Gaussian of inverse width σ, with a typical value of 0.25 $Å^{-1}$, which improves efficiency for computation of eq 3.[55]

In Kv1.2, the "catalytic center" comprises the amino acid triad of F^{233} (S2), E^{236} (S2), and D^{259} (S3) that appears to "catalyze" the transfer of each S4 basic residue across the membrane field, as indicated by recent mutations with natural and unnatural amino acids, electrophysiological recordings, and X-ray crystallography experiments.[56] In the activated VSD, F^{233} "plugs" the most constricted hydrophobic region of the construct and disconnects the internally and externally accessible water crevices. From calculations based on eqs 2 and 3, and applied to Kv1.2, it was demonstrated that a fundamental consequence of the morphology of these high-dielectric regions is to collapse the EP within the VSD, favoring the existence of a focused electric field around the S4 gating charges (Figure 2). Continuum electrostatic computations were initially applied to determine the dimensionless fraction of the membrane voltage V at position r (ϕ_{mp}), according to a modified Poisson–Boltzmann (PB-V) equation that accounts for the effect of transmembrane potential[50]

$$\nabla\cdot[\varepsilon(r)\nabla\phi_{mp}(r)] - \bar{k}^2(r)[\phi_{mp}(r) - \Theta(r)] = 0 \quad (4)$$

where $\varepsilon(r)$ and $\bar{k}(r)$ are the space-dependent dielectric coefficient and Debye–Huckel ionic screening factor, respectively, and $\Theta(r)$ is a Heaviside step function equal to 0 on one side of the membrane and 1 on the other side. Alternatively, explicit all-atom calculations[57,58] were also considered to estimate ϕ_{mp} in the form of the so-called "electrical" distance δ_i[59−62]

$$\delta_i \equiv \frac{\partial}{\partial V}\phi_i|_{V=0} \quad (5)$$

that accounts for the degree of coupling between the local electrostatic potential ϕ_i at position r of the ith protein charge and the TM voltage difference V. ϕ_i was calculated as an average over an ensemble of n MD-generated system configurations; i.e., $\phi_i \equiv (1/n)\sum_{j=1}^{n}\Phi_j(r)$, where $\Phi_j(r)$ is the electrostatic potential, computed according to eq 3. Taken together, both types of calculations were required to show consistently that the membrane voltage profile across the VSD, $\phi_{mp}(z)$, is a sigmoidlike function with its steepest part spanning a narrow TM region (~10–15 Å) in the vicinity of the phenyl center F^{233} (Figure 2). This major finding confirmed the existence of a focused electric field within the activated voltage sensor conformation of Kv1.2.

Modeling the Resting Closed State of Kv1.2. The activated membrane-equilibrated structure of Kv1.2, along with ever-increasing computational power and cutting-edge MD methodologies, has fostered a new generation of in silico studies, focused on channel deactivation, with the main goal of characterizing the structure of the deactivated and/or resting closed state of Kv channels.

Ab Initio Modeling in Combination with MD Simulations. Rosetta is an ab initio structural modeling program initially designed for predicting the structure of soluble proteins but was later adapted to model TM proteins inserted into the phospholipid environment, founded on statistical analyses of TM α-helical data sets.[63] In the method, a fragment-based protein structure generation and a scoring function are combined to predict the structure. Pathak et al. performed the first effort to build up a molecular model of Kv1.2 in the resting closed state by successfully using Rosetta in combination with

dx.doi.org/10.1021/bi3013017 | Biochemistry 2013, 52, 1501−1513

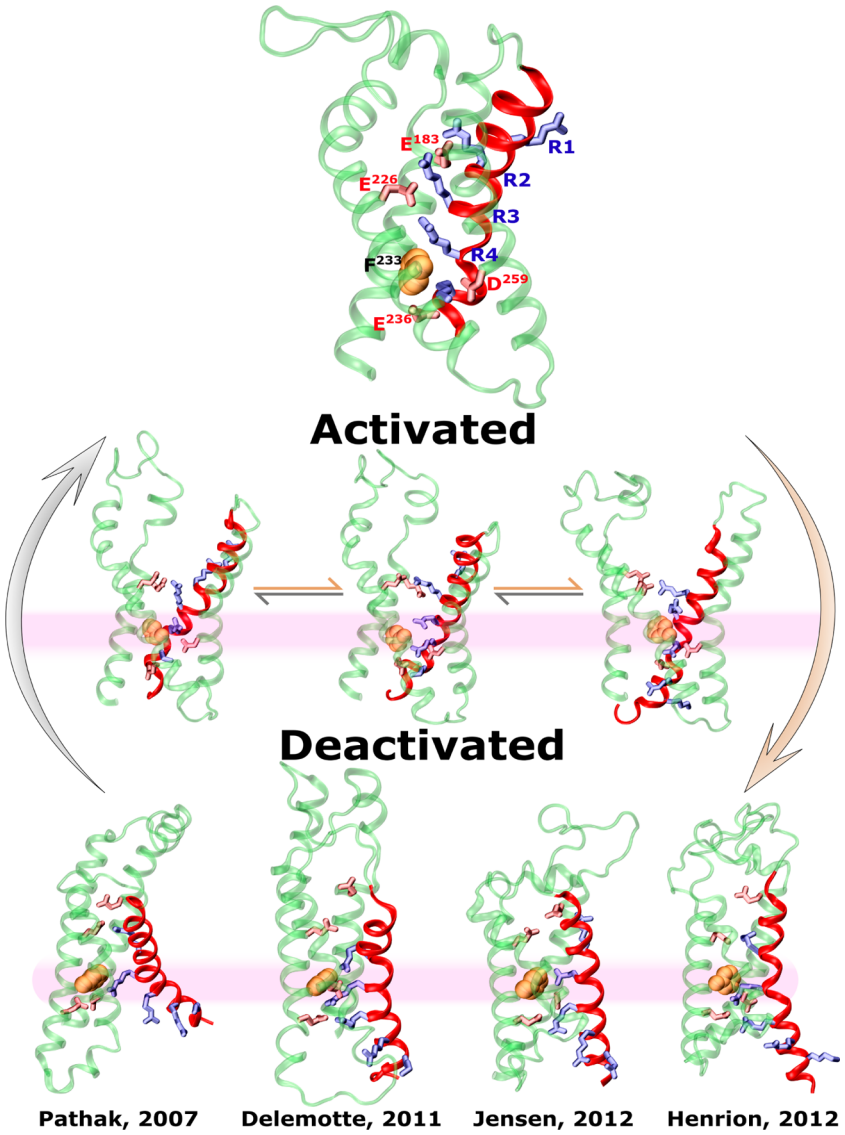

Figure 3. Molecular views of the activated and deactivated VSD structures. S1−S3 are shown as green helices, and S4 is shown as a red helix. The top structure is the activated VSD conformation from the membrane-equilibrated crystal structure shown in ref 38. The bottom structures are proposed models for the deactivated state. From left to right, the assessed S4 displacement throughout deactivation was of approximately 8, 15, 15, and 12 Å, respectively. Despite these differences, the measured gating charges for the models agree with the values of 12−14 e estimated for *Shaker*-like channels (see refs 12−14). The middle structures are three possible VSD intermediates along the activation pathway as described in ref 58. Notice the sliding motion involved in the process and the gradual crossing of arginines past F^{233}.

applied constraints derived from fluorescence scans.[64] More recently, in another study employing Rosetta, Henrion et al. proposed a "C3" resting state model reached via constraints based on experimentally probed metal ion bridges (Cys−Cd^{2+}−Cys and Cys−Cd^{2+}−Glu/Asp) between VSD forming helices of the *Shaker* K^+ channel.[65]

Ab initio modeling is a rather low-resolution technique; as a consequence, it is often followed by MD refinements. In a subsequent study, Khalili-Araghi et al. utilized the resting state model developed by Pathak et al. as an input system for optimization via MD simulations of the channel in an explicit membrane−solvent environment.[66] In view of the relatively low total gating charge identified by Pathak's early model as determined in this simulation, further refinements were then employed to bring S4 to a deeper position within the VSD via steered molecular dynamics (SMD) simulations. Specifically, the authors simulated a nonequilibrium process in which a biasing potential of the form $h[\zeta(t)] = 0.5 \times k[\lambda(x,t) - \zeta(t)]^2$ was used to pull down the S4 charge R_1 along the reaction coordinate $\lambda(x,t)$, corresponding to the TM direction. The biasing potential was coupled to the system with a force constant k of 5 kcal mol^{-1} $Å^{-2}$, moving according to $\zeta(t) = \zeta(0) - vt$ with constant velocity v = 0.5 Å/ns. Note that in SMD one simulates a system with a perturbed Hamiltonian $H(x,t) = H_0(x) + h[\zeta(t)]$ in which $x = x(r,p)$ specifies the position r and momentum p of the system and $H_0(x)$ is the original unperturbed Hamiltonian. This formulation has proven to be very useful for exploring system dynamics along any given reaction coordinate, as considered in refs 67 and 68.

Simulations of Kv1.2 under Applied TM Voltage Differences. The TM electric field is in essence the driving force for the response of Kv1.2 to membrane polarization. Accordingly, in one ambitious set of MD studies, simulators tried to explore the atomic-level time-resolved gating process of

dx.doi.org/10.1021/bi3013017 | *Biochemistry* 2013, 52, 1501−1513

Kv1.2 under applied TM voltage differences, V.[57,58,69−72] For a channel−membrane system, an applied value of V is defined as the difference $\Phi_{int} - \Phi_{ext}$ between the $\Phi(z)$ values at the internal and external system electrolytes; here, $\Phi(z)$ corresponds to the electrostatic potential profile along the membrane normal, and it is computed as the average of the electrostatic potential (see eq 3) over the membrane plane $\rho(z)$ or as a double integral of the charge distribution of all atoms averaged over $\rho(z)$, as $\Phi(z) - \Phi(0) = \int\int \rho(z'')\, dz''\, dz'$.

In these MD studies, two fundamentally different approaches, based on an applied external electric field or charge imbalance protocol, have been employed to reach physiologically relevant ranges of V. In a system composed of a membrane of thickness d and bathed by two disconnected bulk solutions, the experimentally applied voltage results in (i) an effective zero field in the bulk and (ii) a constant electrical field $E = V/d$ across the bilayer. For computer simulations, the electric field E, which will induce the desired range of V, is generated by applying a force F on every charged atom q_i of the system, in such a way that $F = q_iE$. The effectiveness of this method has been demonstrated in pioneering simulations of Kv channels.[73] It is noteworthy that, because of the use of periodic boundary conditions (PBC) in MD simulations, the applied field is rather a function of L_Z, the box size along Z; i.e., $E = V/L_Z$.[74,75] More recently, alternative approaches based on charge imbalance between two disconnected aqueous baths of explicit electrolytes have also been considered in simulation studies.[76,77] In these schemes, the channel−membrane system is bathed with explicit Nernst−Planck ion concentrations and V is imposed on the system by displacing ions from one aqueous compartment to the other, while keeping the overall concentration of the bulk phases constant. Because the system behaves as a condenser, the generated net charge imbalance q_0, between the upper and lower electrolytes, creates V according to the equation $V = q_0/AC$, in which A and C are the membrane area and capacitance, respectively. Because of the use of PBC, special simulation setups based on a twin lipid bilayer system with two bulk phases[76] or on a reduced system with a single bilayer and air−water interfaces on both sides of the membrane have been proposed to impose V via explicit charge imbalance.[77]

In response to an applied voltage, MD simulations limited to time scales of 1 μs succeeded in providing insights into early transition events of the Kv1.2 voltage sensor.[57,69,70,72] The applied voltages were scaled up to 6 times larger than physiological values (~100 mV) to promote a faster response of the system within accessible simulation time scales. Only recently, in one specific simulation, reaching extraordinarily long time scales[71] within the range of hundreds of microseconds, the membrane-equilibrated structure of the Kv1.2−Kv2.1 paddle chimera[37] was shown to be fully deactivated spontaneously in the presence of an applied electric field. The authors of this study benefited from the special-purpose machine designed for high-speed MD simulations (see Molecular Dynamics Simulations). The deactivation process uncovered by this study followed a complex mechanism encompassing many VSD transitions occurring on characteristic time scales, as devised by previous kinetic models describing the time course of gating currents (Figure 3).[78−82] As formerly found in another independent study,[58] in which the VSD deactivation was fully uncovered in a voltage-driven MD simulation combined with SMD, the mechanism was shown to proceed via a downward motion of the S4 basic residues forming sequential and metastable ion pairing with VSD acidic residues and membrane lipid headgroups. Importantly, these simulations also described another key structural modification taking place during deactivation, namely the sequential transfer of the S4 charges across the catalytic center. Naturally, having followed the deactivation mechanism of such channels, both studies from Delemotte et al. and Jensen et al. also proposed models for the resting state of the channel (see below).

Atomistic Models of the VSD Resting State. There are at present several proposed molecular models for the physiologically relevant deactivated or resting closed state of Kv channels (Figure 3). In the model by Pathak et al.,[64] S4 is ~8 Å inwardly positioned relative to its up state; moreover, salt bridge interactions are thought to be formed between R_1 and E^{226} and between R_2 and E^{226} and D^{259}, and R_3 would be slightly below D^{259} while being exposed to intracellular water. The models of Delemotte et al.[58] and Jensen et al.[71] show a larger vertical inward displacement of S4 relative to the up state, i.e., ~15 Å. In these models, R_1 is more deeply embedded within the VSD, satisfying very recent experiments showing its proximity to the catalytic center F^{233} (F^{290} in the Kv1.2−Kv2.1 chimera),[83] and arginines R_2−R_4 are positioned beneath the phenyl center. The model of Delemotte et al. shows further the interaction of R_4 with the lipid PO_4^- headgroups. Finally, in the model by Henrion et al. (C3),[65] the up−down S4 displacement is ~12 Å, and the salt bridge pairs of R_1 and E^{283} (E^{226} in Kv1.2) and R_2 and E^{293} (E^{236} in Kv1.2) above and below the phenyl center, respectively, are said to be formed in the resting state. In the same study, another VSD conformation (C4) thought to be reached solely under enduring hyperpolarized pulses was further considered to match experimental data. In C4, S4 is more deeply located within the domain (~17 Å), favoring interactions between R_1 and E^{293}, all inward to F^{290} (F^{233} in Kv1.2). Importantly, the structures account for much of the experimental data as suggested by a recent analysis investigating the consensual nature of some of the available resting state models.[84]

Structure-Based Computation of Gating Charges (Q). To evaluate the structural robustness and gating activation motions, the aforementioned models were tested against structure-based gating charge measurements. Distinct theoretical methods have been developed to compute gating charge Q associated with the activated open and resting closed conformations of Kv1.2. For instance, Khalili-Araghi et al.[66] have used the "Q-route" to quantify Q in the simulation in which an applied external electric field was used to ensure a constant V. In this formulation, Q is written simply as $Q = \langle Q_d \rangle_{R,V} - \langle Q_d \rangle_{A,V}$,[85] where $\langle Q_d \rangle_{R,V}$ and $\langle Q_d \rangle_{A,V}$ are the ensemble averages of the channel charges in the deactivated and activated conformational states, respectively

$$\langle Q_d \rangle_{s,V} = \left\langle \sum_{i=1}^{N} q_i \frac{z_i^u}{L_Z} \right\rangle_{s,V} \quad (6)$$

where L_Z is the size of the simulation box along the Z axis, normal to the bilayer, and q_i and Z_i are the partial charge of atom i and its unwrapped coordinate along Z, respectively. Alternatively, the "direct measurement" was used by Delemotte et al. to compute Q in the Kv1.2 simulations in which the charge imbalance protocol was used to apply V.[57,58] In this approach, the charge imbalance across the membrane due to protein charges in a given conformation is linearly related to V, so that

$$q_0^{\text{protein}}(t) = -q_0^{\text{ion}}(t) + ACV(t) \quad (7)$$

where q_0^{protein} and q_0^{ion} are the contributions of protein charges and ions, respectively, to the total charge imbalance $q_0(t) = q_0^{\text{protein}}(t) + q_0^{\text{ion}}(t)$, A is the membrane area, and C is the membrane capacitance, which is constant for the channel–membrane system[86] and amounts to ~0.9 μF/cm^2, as measured from MD simulations.[57] Accordingly, Q associated with two conformations of the channel, λ_1 and λ_2, can be thus obtained as

$$Q = -\frac{1}{2}[q_0^{\text{protein}}(\lambda_2) - q_0^{\text{protein}}(\lambda_1)] \quad (8)$$

where $q_0^{\text{protein}}(\lambda_1)$ and $q_0^{\text{protein}}(\lambda_2)$ are the charge imbalance due to protein charges in λ_1 and λ_2, respectively. Finally, a more general and free energy-based approach, the "G-route",[85] was also used in different publications to make concrete connections between the models and experiments.[50,57,58,61,62,66,71,87,88] In this calculation, Q is linked to the microscopic state of the channel through

$$Q = \frac{\Delta G(\lambda_2, V) - \Delta G(\lambda_1, V)}{V} \quad (9)$$

where, for each λ conformation, $\Delta G(\lambda,V)$ is the excess free energy of the channel due to the applied voltage. It relates the conformation of the channel to $\phi_{\text{mp}}(i)$

$$\Delta G(\lambda, V) = G(\lambda, V) - G(\lambda, 0) = V\sum_i q_i \phi_{\text{mp}}^{\lambda}(i) \quad (10)$$

which represents the coupling of the ith channel charge q_i to the transmembrane potential. In practice, for a given conformation of the channel, $\phi_{\text{mp}}^{\lambda}(i)$ has been estimated following different strategies: (i) by means of a continuum electrostatic approximation based on the Poisson–Boltzmann equation modified to account for the effect of the transmembrane voltage (eq 4),[50,61] (ii) by means of perturbation MD simulations as the charging free energy of q_i at two different voltages,[66,71,85] and (iii) alternatively in the so-called "energetic formalism" approach,[57] a less time-costly computation of $\phi_{\text{mp}}^{\lambda}(i)$ that can also be obtained in the form of the "electrical distance" (eq 5).[61,62] It is noteworthy that within the framework of the Ramo–Schokley theorem, Q could also be expressed as a function of starting and ending locations of all particles bearing charges q_i and $\phi_i^{\lambda}(r)$, which is another formulation identical to that following eqs 9 and 10.[89]

When tested against experimental estimates of Q measurements for *Shaker*-like channels (12–14 e), the resting closed models of Kv1.2 (or the Kv1.2–Kv2.1 paddle chimera) were all found to be in fine agreement with the experimental assessments.[12−14] With the Q route and direct measurement, the formal free energy approach was particularly advantageous, allowing the identification of several S2–S3 negatively charged residues along with the S4 basic residues that contribute to the Kv1.2 gating charges as well as quantification of their specific contributions to Q. These results are consistent with experiments showing that mutations of the S2–S3 and S4 residues influence Q.[13,86,90−93]

Emerging Picture for VSD Activation. The same general electric properties determined for the activated open conformation of Kv1.2 (see above) were also found when analyzing a resting VSD model,[58] suggesting that the electric field within the domain is not drastically reshaped during its structural transition. This result was of particular interest, given the long-lasting controversy concerning the "static" or "remodeled" nature of the electric field in VGCCs. Currently, though not refuting key features of the paddle or transporter models, i.e., the S3b–S4 forming paddle, hydration of the VSD and field focalization, the emerging picture from the Kv1.2 structure and its manifold studies depicts major characteristics of the sliding helix model. Accordingly, S4 moves from 10 to 15 Å in the TM direction throughout activation, traversing its own protein-lined pathway and forming conformation-dependent salt bridges between its basic residues and neighboring countercharges.[94]

Pore Opening and Coupling with the VSD. The structural studies of Kv channels indicate so far that pore opening involves transient hydration of the ionic conduction pathway, allowing the diffusion of ions throughout a hydrophilic environment, such as that encountered in the open gate of Kv1.2.[38] Here, sophisticated free energy calculations were integral to the study of the energetics of ion conduction through the channel. These calculations were made with the free energy profile or potential of mean force (PMF). The PMF along any given reaction coordinate λ is related to the equilibrium probability density $P(\lambda)$:

$$G(\lambda) = -\frac{1}{\beta} \ln P(\lambda) + G_0 \quad (11)$$

where $\beta^{-1} = kT$, $G(\lambda)$ is the free energy of the state defined by a specific value of λ, and G_0 is a constant. A detailed description of the vast repertoire of free energy methods in the context of MD simulations can be found in refs 95 and 96.

In one of the first approaches, Beckstein et al. have used umbrella sampling with the weighted histogram analysis method (WHAM) to estimate the $G(\lambda)$ profile for ion permeation through nanopore models with various radii.[97] In their approach, an external potential of the form $U(\lambda) = k/2(\lambda - \lambda_i)^2$, typically used in the method, was employed to efficiently bias the equilibrium distribution of the ion along the permeation pathway λ. In practice, this was done following a stratification approach by performing several independent simulations with the ion initially positioned at different λ_i values. From each of these simulations, the WHAM method was then used to reconstruct the unbiased density $P_i(\lambda)$ from the biased one, with the main goal of combining all $P_i(\lambda)$ values into the equilibrium probability density $P(\lambda)$, from which the PMF was computed according to eq 11. Later, using MD simulations and the adaptive-biasing-force (ABF) method,[98,99] Treptow and Tarek estimated the PMF of ion conduction through the more complex activation gate of Kv1.2.[100] The method corresponds to the usual thermodynamic integration (TI) scheme (eq 12), except for the explicit dependence on the volume element in generalized coordinates.

$$\frac{dG(\lambda)}{d\lambda} = \left\langle \frac{\partial U(r^N)}{\partial \lambda} \right\rangle_{\lambda} = -\langle F_{\lambda} \rangle_{\lambda} \quad (12)$$

The ABF method computes the mean force $\langle F_{\lambda} \rangle_{\lambda}$ at a given position of λ by applying an iterative biasing force F^{ABF} that allows the system to overcome free energy barriers. As the estimation of $\langle F_{\lambda} \rangle_{\lambda}$ is improved during the simulation, it adapts to match precisely the free energy barrier, promoting a uniform sampling by diffusing the system on a flat energy surface. In their computation, authors have evaluated the PMFs for ion conduction over a pathway of 27 Å, ranging from the cytoplasmic entrance of the pore to the central cavity of the

channel, and a stratification of nine windows was adopted to minimize statistical errors. A homogeneous sampling along the reaction coordinate, in which at least 20000 values of the force were collected for averaging, ensured convergence of the PMF.

These free energy calculations showed independently that narrowing of a hydrophobic gate dehydrates the permeation pathway, restraining ion diffusion (Figure 4).[97,100] Computa-

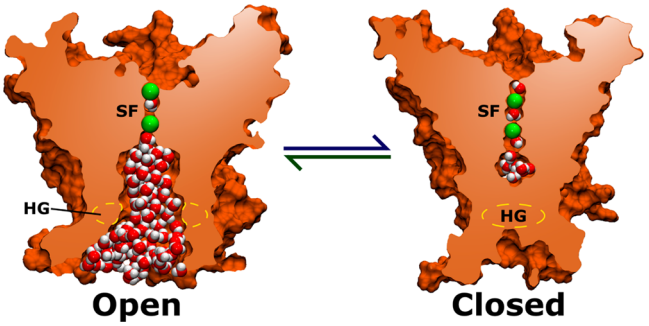

Figure 4. Pore narrowing and dehydration at the hydrophobic gate stop the ionic flow. The intrinsic pore gating mechanism acts via constriction of the hydrophobic gate and leads to dehydration of the ionic permeation pathway. Abbreviations: HG, hydrophobic gate; SF, selectivity filter.

tions based on the finite difference Poisson–Boltzmann equation (eq 2) have pointed out that the free energy barrier for conduction results from the reaction field energy, corresponding essentially to a dehydration penalty.[54,97] The reaction field energy is the difference between the electrostatic energies of the channel with the permeating ion and the ion far away in bulk. Overall, as demonstrated by such structural studies, hydrophobic gates act as efficient devices in the control of ion transport. In fact, a number of other ion channels also present hydrophobic gates: nicotinic receptors,[101] the bacterial mechanosensitive MscS channel,[102] K_{2P} channels,[103] and NaChBac.[104] Furthermore, hydrophobic gates seem to equip the channel pore with an intrinsic gating mechanism, qualifying the construct to operate autonomously. Indeed, recent microsecond-long MD simulations of rat Kv1.2 showed that, starting from an open conformation, the pore region may go through a dewetting transition, followed by channel closing by means of an intrinsic hydrophobic gating mechanism.[105] Dewetting results from capillary evaporation alternated with capillary condensation of water within the pore, which is a common feature of hydrophobic nanopores in general.[106]

A major question of how the electrically driven or dewetting-driven motions of VSD and PD could be joined cooperatively to generate the open–closed transitions of the entire channel arises. While easily viewed as two autonomic operating devices, the pore and the VSD cast a synergistic functional machine. So far, this matter has been approached via site-directed mutations, revealing that the S4–S5 linker residues took part in such a process.[107−110] Only recently have long molecular dynamics simulations provided the very first structural and dynamical insights on the subject (Figure 5). Jensen et al. studied the deactivation and activation pathways of the Kv1.2–Kv2.1 paddle chimera channel.[71] As indicated by the simulation, activation follows a well-described path: starting from a closed deactivated state, depolarization-driven S4 upward displacements occur along with a final cooperative S4 motion to bring the S4–S5 linker to a tense conformation. This tension results

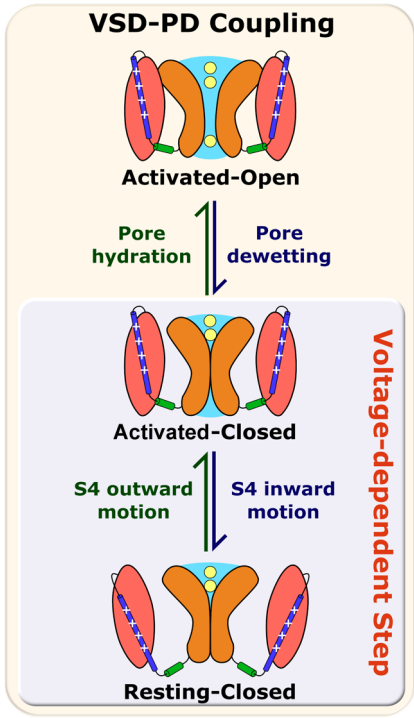

Figure 5. Schematic representation of the voltage sensor–pore coupling during K^+ channel gating, as revealed by the extremely long molecular dynamics simulation of ref 71.

in perturbation and weakening of the linker–S6 interaction, permitting, at first, opening of the pore lower gate accompanied by partial pore hydration; ions then enter the cavity, inducing progressive rehydration of the conducting pore along with complete pore opening. The deactivation event follows somewhat the reverse path: under hyperpolarization, an early downward movement of S4 precedes pore dewetting and its subsequent collapse. Only after complete pore closure does VSD reach a fully down state. Also, the simulation illustrates that to complete the pore opening process, all four VSDs are required to be fully activated. Closing, on the other hand, solely requires rearrangements of a single VSD. Despite the detailed description of the pathway unveiled for the Kv1.2–Kv2.1 chimera, the matter is still under discussion for other channels such as KCNQ1, for which it is proposed that activation results from sequential transitions unconditioned to a concerted motion of all four VSDs.[111] KCNQ1 illustrates the role sequence diversity may have in generating potentially different mechanisms between the various channels

FUTURE DIRECTIONS

After more than 50 years of study and with the aforementioned models in mind, one major challenge is to place all the structural and functional data into a unified framework so it can be applied to other appealing topics.

Toward other VGCCs. In 2011, the X-ray structure of a voltage-gated sodium channel from the bacterium *Arcobacter butzleri*, NavAb, was determined at 2.7 Å,[6] featuring a closed PD and the four VSDs seemingly activated (Figure 1). The structure, which was interpreted as being representative of the pre-open state of the channel, has offered the first high-resolution structural template available for the investigation of other much less frequently studied Na^+ and Ca^{2+} channels. Because of their structural similarity, members of the VGCC

dx.doi.org/10.1021/bi3013017 | *Biochemistry* 2013, 52, 1501–1513

family are expected to exhibit a voltage sensing and gating mechanism similar to those discovered in Kv1.2. Large variations might exist for some specific channels, such as the HCN channel, for which the S4-mediated process follows an opposite voltage dependence.[112] For NavAb and related bacterial channels, results from site-directed spin labeling and EPR spectroscopy support the notion that its voltage sensing pathway may be highly similar to several K^+ channels.[113] Therefore, established experimental and theoretical approaches can be applied to characterize the active and resting states of NavAb and to elucidate the structural similarities and divergence between them. As described in the following, this proposition has been strengthened with recent publications.

On the basis of the analysis of disulfide locking of Cys double mutants, Catterall and co-workers have described an extensive set of state-dependent interactions between S4 charges and their countercharged residues in neighboring VSD segments for the orthologous NaChBac channel. By using the Rosetta method, authors have combined the set of interactions with structural data available for related channels, including the Kv1.2−Kv2.1 chimera and NavAb, to construct structural models of resting, intermediate, and activated states of NaChBac.[27] In another recent study, Amaral et al. considered two specific structures of Kv1.2, in the activated open[49] and resting closed[58] conformations, as guide templates to drive a series of biased and equilibrium MD simulations that aimed to explore the activation open pathway of NavAb.[114] The biasing simulations were accomplished by means of target molecular dynamics (TMD),[115] in which a selection of N atoms of the channel was guided to the reference structures by an applied potential $U_{TMD} = {}^1/_2(k/N)[\mathrm{rmsd}(t) - \mathrm{rmsd}^*(t)]^2$, with root-mean-square deviations $\mathrm{rmsd}(t)$ and $\mathrm{rmsd}^*(t)$ corresponding to instantaneous and target deviations between structures, respectively. Specifically, by using a force constant k of 4.5 kcal mol^{-1} Å^{-2} and a velocity of 0.25 Å/ns for the target deviation $\mathrm{rmsd}^*(t)$, authors have sampled channel conformations potentially related to the resting closed and activated open states, a result strongly consistent with the recently published X-ray crystal structures of the orthologous channels NavRh[8] and NavMs.[9]

In many instances, acquisition of structural data for different members of the superfamily of K^+ and Na^+ channels is highly desirable and actually required to extend our knowledge on other appealing topics. In this context, the X-ray structures and atomistic models available for distinct conformations of Kv1.2, NavAb, and other channels provide a valuable set of templates that can be further aided by comparative protein modeling to built-up models of structurally unknown channels. Consistent with this notion, homology models for the TM domain of K-Shaw[116] and the VSD of the mammalian Nav1.4 channel[117] have been successfully built and recently considered in studying the regulation and dysfunction of VGCCs (see below). The success of these approaches templated on Kv1.2 and NavAb relied on the significant level of sequence similarity shared by channels within the TM segments.

Structural Details of the Inactivation State. Inactivation is another voltage-dependent process involving complex structural rearrangements of VGCCs, ultimately hindering the passage of ions through the channel. To date, key aspects of this process have been unveiled for K^+ channels, indicating that these rearrangements are described by two main mechanisms: a fast inactivation occurring on the millisecond time scale and a slow, or C-type, inactivation occurring under lingering depolarized conditions or repetitive firing of potentials. The fast inactivation relates to the clogging of the intracellular opening of the pore by the N-terminus of the channel.[118] Metadynamics MD simulations,[119] and subsequent experiments,[120] revealed that slow inactivation is achieved through structural defects in the selectivity filter, leading to unusual dihedral angle conformations. Whether the hydrophobic gating mechanism described for the pore of Kv1.2 (see above) corresponds as well to an intrinsic inactivation mechanism in Kv channels remains to be validated.

In this regard, much is still unanswered when it comes to structural details of the inactivation mechanisms of sodium channels. For the mammalian Nav channels, the fast inactivation has been shown to occur via a "hinged lid" mechanism performed by an intracellular inactivation gate that binds to the mouth of the pore, whereas the slow inactivation is much more poorly characterized.[121] For bacterial Nav channels, which do not present the mammalian relative inactivation machinery, a variant inactivation is likely to derive from closure of the intracellular gate of the main pore,[122−126] which seems to be similar to the hydrophobic gating mechanism described for Kv1.2. Indeed, the X-ray structures of NavAb[7] and NavRh,[8] featuring a closed PD, have recently been described as potentially inactivated structures of the channel. As previously highlighted, a detailed characterization of fully activated−inactivated structures, and even the pathway by which the transition is accomplished, are significant in terms of a more profound understanding of other fundamental topics such as conduction and channel modulation by ligands.

Channel Modulation. Another fascinating topic relates to the modulation of voltage-gated channels (VGCs). This subject concerns the possibility of investigating how ligands such as divalent cations, peptides, free sulfhydryl modifiers, general and local anesthetics, and toxins may alter VGCC function. Indeed, a series of studies have already been, and are still being, conducted in this regard. For instance, in a recent study, alanine scanning experiments along with MD docking calculations succeeded in identifying binding sites for inhaled anesthetics both at the S4−S5 linker and at the activation gate of K-Shaw.[116] Moreover, other structural studies were also conducted to investigate the functional and structural effects engendered by pore-blocking toxins[127] and gating modifier peptides[128] binding to VGCCs. In light of this scenario and the just released sodium channel structures, studies with these template structures are thought to be of great value for further investigations of binding of the ligand to VGCCs. In fact, the anesthetic sensitivity of NavAb-related channels, such as NaChBac,[129] suggests that NavAb is a useful model for studies of the action of general anesthetics. Furthermore, given the key role of Nav channels in generating the upstroke of the action potential, toxins act at six or more distinct receptor sites on these channels compared to only two sites on Kv.[130]

Channel Dysfunctions. Finally, in view of the great structural progress that has been made so far, we are reaching a critical point where it is possible to tackle more intricate and relevant questions, such as the molecular origins of VGCC-related dysfunctions. It is remarkable that such a deep issue can be investigated in the context of atomic-level structural studies. A series of recent MD investigations[71,131,132] address the interplay between S4 helix mutations and inheritable channelopathies, e.g., epilepsy, paralyses, and long QT syndrome. By considering the Kv1.2 channel, these studies demonstrated that specific S4 mutations disarrange the VSD

dx.doi.org/10.1021/bi3013017 | Biochemistry 2013, 52, 1501−1513

electrostatic network, giving rise to leakage of cations, the so-called "omega" or "gating pore" currents,[133,134] through an off-pore conduction pathway within the voltage sensor domain. Here, similar studies yet to be conducted on sodium channels will likely be very instructive in understanding the molecular properties underlying inheritable genetic diseases. In this direction, initial modeling efforts have suggested that the hydrophobic septum that isolates the intracellular and extracellular media within the VSDs of Nav1.4 is ~2 Å long, which is similar to the length of that encountered in the VSD of Kv channels.[117] This structural pattern rationalizes the existence of gating pore currents on the Nav1.4 channel.

AUTHOR INFORMATION

Corresponding Author

*Laboratório de Biofísica Teórica e Computacional, Departamento de Biologia Celular, Universidade de Brasília, Campus Darcy Ribeiro, Brasília, DF, Brazil, CEP 70910-900. E-mail: treptow@unb.br. Phone: +55.61.3107.3098.

Author Contributions

L.S. and C.S. contributed equally to this work.

Funding

W.T. thanks the National Council of Technological and Scientific Development (CNPq) for research support (Grant 470406/2011-9) and graduate fellowships to L.S. and C.S.

Notes

The authors declare no competing financial interest.

ACKNOWLEDGMENTS

We thank Dr. M. Jensen, Dr. V. Carnevale, and E. Palovcak for useful comments on an early version of the manuscript.

REFERENCES

(1) Hille, B. (1992) *Ionic channels of excitable membranes*, 2nd ed., Sinauer, Sunderland, MA.

(2) Lehmann-Horn, F., and Jurkat-Rott, K. (1999) Voltage-Gated Ion Channels and Hereditary Disease. *Physiol. Rev. 79*, 1317−1372.

(3) Mantegazza, M., Curia, G., Biagini, G., Ragsdale, D. S., and Avoli, M. (2010) Voltage-gated sodium channels as therapeutic targets in epilepsy and other neurological disorders. *Lancet Neurol. 9*, 413−424.

(4) Bezanilla, F. (2000) The voltage sensor in voltage-dependent ion channels. *Physiol. Rev. 80*, 555−592.

(5) Horn, R. (2000) Conversation between voltage sensors and gates of ion channels. *Biochemistry 39*, 15653−15658.

(6) Payandeh, J., Scheuer, T., Zheng, N., and Catterall, W. A. (2011) The crystal structure of a voltage-gated sodium channel. *Nature 475*, 353−358.

(7) Payandeh, J., El-Din, T. M. G., Scheuer, T., Zheng, N., and Catterall, W. A. (2012) Crystal structure of a voltage-gated sodium channel in two potentially inactivated states. *Nature 486*, 135−139.

(8) Zhang, X., Ren, W., DeCaen, P., Yan, C., Tao, X., Tang, L., Wang, J., Hasegawa, K., Kumasaka, T., He, J., Wang, J., Clapham, D. E., and Yan, N. (2012) Crystal structure of an orthologue of the NaChBac voltage-gated sodium channel. *Nature 486*, 130−134.

(9) McCusker, E. C., Bagnéris, C., Naylor, C. E., Cole, A. R., D'Avanzo, N., Nichols, C. G., and Wallace, B. A. (2012) Structure of a bacterial voltage-gated sodium channel pore reveals mechanisms of opening and closing. *Nat. Commun. 3*, 1102.

(10) Sakmann, B., and Neher, E. (1984) Patch clamp techniques for studying ionic channels in excitable membranes. *Annu. Rev. Physiol. 46*, 455−472.

(11) Hodgkin, A. L., and Huxley, A. F. (1952) The components of membrane conductance in the giant axon of Loligo. *J. Physiol. 116*, 473−496.

(12) Schoppa, N. E., McCormack, K., Tanouye, M. A., and Sigworth, F. J. (1992) The size of gating charge in wild-type and mutant Shaker potassium channels. *Science 255*, 1712−1715.

(13) Aggarwal, S. K., and MacKinnon, R. (1996) Contribution of the S4 segment to gating charge in the Shaker K channel. *Neuron 16*, 1169−1177.

(14) Seoh, S. A., Sigg, D., Papazian, D. M., and Bezanilla, F. (1996) Voltage-sensing residues in the S2 and S4 segments of the Shaker K^+ channel. *Neuron 16*, 1159−1167.

(15) Noda, M., Shimizu, S., Tanabe, T., Takai, T., Kayano, T., Ikeda, T., Takahashi, H., Nakayama, H., Kanaoka, Y., and Minamino, N. (1984) Primary structure of *Electrophorus electricus* sodium channel deduced from cDNA sequence. *Nature 312*, 121−127.

(16) Tempel, B. L., Papazian, D. M., Schwarz, T. L., Jan, Y. N., and Jan, L. Y. (1987) Sequence of a probable potassium channel component encoded at Shaker locus of *Drosophila*. *Science 237*, 770−775.

(17) Islas, L. D., and Sigworth, F. J. (1999) Voltage sensitivity and gating charge in Shaker and Shab family potassium channels. *J. Gen. Physiol. 114*, 723−742.

(18) Yang, N., George, A. L. J., and Horn, R. (1996) Molecular basis of charge movement in voltage-gated sodium channels. *Neuron 16*, 113−122.

(19) Larsson, H. P., Baker, O. S., Dhillon, D. S., and Isacoff, E. Y. (1996) Transmembrane movement of the Shaker K^+ Channel S4. *Neuron 16*, 387−397.

(20) Starace, D. M., Stefani, E., and Bezanilla, F. (1997) Voltage-dependent proton transport by the voltage sensor of the Shaker K^+ channel. *Neuron 19*, 1319−1327.

(21) Mannuzzu, L. M., Moronne, M. M., and Isaccoff, E. Y. (1996) Direct physical measurement of conformational rearrangement underlying potassium channel gating. *Science 271*, 213−216.

(22) Papazian, D. M., Shao, X. M., Seoh, S.-A., Mock, A. F., Huang, Y., and Wainstock, D. H. (1995) Electrostatic interactions of S4 voltage sensor in Shaker K^+ channel. *Neuron 14*, 1293−1301.

(23) Tiwari-Woodruff, S. K., Schulteis, C. T., Mock, A. F., and Papazian, D. M. (1997) Electrostatic interactions between transmembrane segments mediate folding of Shaker K^+ channel subunits. *Biophys. J. 72*, 1489−1500.

(24) Wu, D., Delaloye, K., Zaydman, M. A., Nekouzadeh, A., Rudy, Y., and Cui, J. (2010) State-dependent electrostatic interactions of S4 arginines with E1 in S2 during Kv7.1 activation. *J. Gen. Physiol. 135*, 595−606.

(25) DeCaen, P. G., Yarov-Yarovoy, V., Sharp, E. M., Scheuer, T., and Catterall, W. A. (2009) Sequential formation of ion pairs during activation of a sodium channel voltage sensor. *Proc. Natl. Acad. Sci. U.S.A. 106*, 22498−22503.

(26) DeCaen, P. G., Yarov-Yarovoy, V., Scheuer, T., and Catterall, W. A. (2011) Gating charge interactions with the S1 segment during activation of a Na^+ channel voltage sensor. *Proc. Natl. Acad. Sci. U.S.A. 108*, 18825−18830.

(27) Yarov-Yarovoy, V., DeCaen, P. G., Westenbroek, R. E., Pan, C.-Y., Scheuer, T., Baker, D., and Catterall, W. A. (2012) Structural basis for gating charge movement in the voltage sensor of a sodium channel. *Proc. Natl. Acad. Sci. U.S.A. 109*, E93−E102.

(28) Blaustein, R. O., and Miller, C. (2004) Ion channels: Shake, rattle or roll? *Nature 427*, 499−500.

(29) Guy, H. R., and Seetharamulu, P. (1986) Molecular model of the action potential sodium channel. *Proc. Natl. Acad. Sci. U.S.A. 83*, 508−512.

(30) Catterall, W. A. (1986) Voltage-dependent gating of sodium channels: Correlating structure and function. *Trends Neurosci. 9*, 7−10.

(31) Keynes, R. D., and Elinder, F. (1999) The screw-helical voltage gating of ion channels. *Proc. Biol. Sci. 266*, 843−852.

(32) Gandhi, C. S., and Isacoff, E. Y. (2002) Molecular Models of Voltage Sensing. *J. Gen. Physiol. 120*, 455−463.

(33) Cha, A., Ruben, P. C., George, A. L., Fujimoto, E., and Bezanilla, F. (1999) Atomic scale movement of the voltage-sensing region in a potassium channel measured via spectroscopy. *Nature 402*, 813−817.

(34) Starace, D. M., and Bezanilla, F. (2004) A proton pore in a potassium channel voltage sensor reveals a focused electric field. *Nature 427*, 548−553.
(35) Posson, D. J., Ge, P., Miller, C., Bezanilla, F., and Selvin, P. R. (2005) Small vertical movement of a K^+ channel voltage sensor measured with luminescence energy transfer. *Nature 436*, 848−851.
(36) Jiang, Y., Lee, A., Chen, J., Ruta, V., Cadene, M., Chait, B. T., and MacKinnon, R. (2003) X-ray structure of a voltage-dependent K^+ channel. *Nature 423*, 33−41.
(37) Long, S. B., Tao, X., Campbell, E. B., and MacKinnon, R. (2007) Atomic structure of a voltage-dependent K^+ channel in a lipid membrane-like environment. *Nature 450*, 376−382.
(38) Long, S. B., Campbell, E. B., and MacKinnon, R. (2005) Crystal structure of a mammalian voltage-dependent Shaker family K^+ channel. *Science 309*, 897−903.
(39) Ingólfsson, H. I., Li, Y., Vostrikov, V. V., Gu, H., Hinton, J. F., Koeppe, R. E., Roux, B., and Andersen, O. S. (2011) Gramicidin A backbone and side chain dynamics evaluated by molecular dynamics simulations and nuclear magnetic resonance experiments. I: Molecular dynamics simulations. *J. Phys. Chem. B 115*, 7417−7426.
(40) Frenkel, D., and Smit, B. (2001) *Understanding Molecular Simulation, Second Edition: From Algorithms to Applications*, Academic Press, San Diego.
(41) MacKerell, A. D., Jr., Bashford, D., Bellott, M., Dunbrack, R. L., Jr., Evanseck, J., Field, M. J., Fischer, S., Gao, J., Guo, H., Ha, S., Joseph-McCarthy, D., Kuchnir, L., Kuczera, K., Lau, F. T. K., Mattos, C., Michnick, S., Ngo, T., Nguyen, D. T., Prodhom, B., Reiher, W. E., III, Roux, B., Schlenkrich, M., Smith, J. C., Stote, R., Straub, J., Watanabe, M., Wiorkiewicz-Kuczera, J., Yin, D., and Karplus, M. (1998) All-atom empirical potential for molecular modeling and dynamics studies of proteins. *J. Phys. Chem. B 102*, 3586−3616.
(42) MacKerell, A. D., Jr., Feig, M., and Brooks, C. L., III (2004) Improved Treatment of the Protein Backbone in Empirical Force Fields. *J. Am. Chem. Soc. 126*, 698−699.
(43) Cornell, W., Cieplak, P., Bayly, C., Gould, I., Merz, K., Ferguson, D., Spellmeyer, D., Fox, T., Caldwell, J., and Kollman, P. (1995) A Second Generation Force Field for the Simulation of Proteins, Nucleic Acids, and Organic Molecules. *J. Am. Chem. Soc. 117*, 5179−5197.
(44) Schmid, N., Eichenberger, A. P., Choutko, A., Riniker, S., Winger, M., Mark, A. E., and Van Gunsteren, W. F. (2011) Definition and testing of the GROMOS force-field versions 54A7 and 54B7. *Eur. Biophys. J. 40*, 843−856.
(45) Ponder, J. W., and Case, D. A. (2003) Force fields for protein simulations. *Adv. Protein Chem. 66*, 27−85.
(46) Phillips, J. C., Braun, R., Wang, W., Gumbart, J., Tajkhorshid, E., Villa, E., Chipot, C., Skeel, R. D., Kale, L., and Schulten, K. (2005) Scalable molecular dynamics with NAMD. *J. Comput. Chem. 26*, 1781−1802.
(47) Van Der Spoel, D., Lindahl, E., Hess, B., Groenhof, G., Mark, A. E., and Berendsen, H. J. C. (2005) GROMACS: Fast, flexible, and free. *J. Comput. Chem. 26*, 1701−1718.
(48) Shaw, D., Deneroff, M., Dror, R., Kuskin, J., Larson, R., Salmon, J., Young, C., Batson, B., Bowers, K., Chao, J., Eastwood, M., Gagliardo, J., Grossman, J., Ho, R., Ierardi, D., Kolossváry, I., Klepeis, J., Layman, T., McLeavey, C., Moraes, M., Mueller, R., Priest, E., Shan, Y., Spengler, J., Theobald, M., Towles, B., and Wang, S. (2007) Anton, a special-purpose machine for molecular dynamics simulation. *Proceedings of the 34th Annual International Symposium on Computer Architecture* , 1−12.
(49) Treptow, W., and Tarek, M. (2006) Environment of the gating charges in the Kv1.2 Shaker potassium channel. *Biophys. J. 90*, L64−L66.
(50) Jogini, V., and Roux, B. (2007) Dynamics of the Kv1.2 voltage-gated K^+ channel in a membrane environment. *Biophys. J. 93*, 3070−3082.
(51) Kobertz, W. R., and Miler, C. (1999) K^+ channels lacking the "tetramerization" domain: Implications for pore structure. *Nat. Struct. Biol. 6*, 1122−1125.
(52) Sands, Z. A., and Sansom, M. S. (2007) How does a voltage sensor interact with a lipid bilayer? Simulations of a potassium channel domain. *Structure 15*, 235−244.
(53) Krepkiy, D., Mihailescu, M., Freites, J. A., Schow, E. V., Worcester, D. L., Gawrisch, K., Tobias, D. J., White, S. H., and Swartz, K. J. (2009) Structure and hydration of membranes embedded with voltage-sensing domains. *Nature 462*, 473−479.
(54) Jogini, V., and Roux, B. (2005) Electrostatics of the intracellular vestibule of K^+ channels. *J. Mol. Biol. 354*, 272−288.
(55) Aksimentiev, A., and Schulten, K. (2005) Imaging α-hemolysin with molecular dynamics: Ionic conductance, osmotic permeability, and the electrostatic potential map. *Biophys. J. 88*, 3745−3761.
(56) Tao, X., Lee, A., Limapichat, W., Dougherty, D. A., and MacKinnon, R. (2010) A gating charge transfer center in voltage sensors. *Science 328*, 67−73.
(57) Treptow, W., Tarek, M., and Klein, M. L. (2009) Initial response of the potassium channel voltage sensor to a transmembrane potential. *J. Am. Chem. Soc. 131*, 2107−2109.
(58) Delemotte, L., Tarek, M., Klein, M. L., Amaral, C., and Treptow, W. (2011) Intermediate states of the Kv1.2 voltage sensor from atomistic molecular dynamics simulations. *Proc. Natl. Acad. Sci. U.S.A. 108*, 6109−6114.
(59) Stevens, C. F. (1978) Interactions between intrinsic membrane protein and electric field. An approach to studying nerve excitability. *Biophys. J. 22*, 295−306.
(60) Sigworth, F. J. (1994) Voltage gating of ion channels. *Q. Rev. Biophys. 27*, 1−40.
(61) Roux, B. (1997) Influence of the membrane potential on the free energy of an intrinsic protein. *Biophys. J. 73*, 2980−2989.
(62) Islas, L. D., and Sigworth, F. J. (2001) Electrostatic and the gating pore of Shaker potassium channels. *J. Gen. Physiol. 117*, 69−89.
(63) Yarov-Yarovoy, V., Schonbrun, J., and Baker, D. (2006) Multipass membrane protein structure prediction using Rosetta. *Proteins 62*, 1010−1025.
(64) Pathak, M. M., Yarov-Yarovoy, V., Agarwal, G., Roux, B., Barth, P., Kohout, S., Tombola, F., and Isacoff, E. Y. (2007) Closing in on the resting state of the shaker K^+ channel. *Neuron 56*, 124−140.
(65) Henrion, U., Renhorn, J., Börjesson, S. I., Nelson, E. M., Schwaiger, C. S., Bjelkmar, P., Wallner, B., Lindahl, E., and Elinder, F. (2012) Tracking a complete voltage-sensor cycle with metal-ion bridges. *Proc. Natl. Acad. Sci. U.S.A.*, DOI:10.1073/pnas.1116938109.
(66) Khalili-Araghi, F., Jogini, V., Yarov-Yarovoy, V., Tajkhorshid, E., Roux, B., and Schulten, K. (2010) Calculation of the gating charge for the Kv1.2 voltage-activated potassium channel. *Biophys. J. 98*, 2189−2198.
(67) Jensen, M. U., Park, S., Tajkhorshid, E., and Schulten, K. (2002) Energetics of glycerol conduction through aquaglyceroporin GlpF. *Proc. Natl. Acad. Sci. U.S.A. 99*, 6731−6736.
(68) Treptow, W., and Tarek, M. (2006) K^+ conduction in the selectivity filter of potassium channels is monitored by the charge distribution along their sequence. *Biophys. J. 91*, L81−L83.
(69) Nishizawa, M., and Nishizawa, K. (2008) Molecular dynamics simulation of Kv channel voltage sensor helix in a lipid membrane with applied electric field. *Biophys. J. 95*, 1729−1744.
(70) Bjelkmar, P., Niemelä, P. S., Vattulainen, I., and Lindahl, E. (2009) Conformational changes and slow dynamics through microsecond polarized atomistic molecular simulation of an integral Kv1.2 ion channel. *PLoS Comput. Biol. 5*, e1000289.
(71) Jensen, M. Ø., Jogini, V., Borhani, D. W., Leffler, A. E., Dror, R. O., and Shaw, D. E. (2012) Mechanism of Voltage Gating in Potassium Channels. *Science 336*, 229−233.
(72) Denning, E. J., Crozier, P. S., Sachs, J. N., and Woolf, T. B. (2009) From the gating charge response to pore domain movement: Initial motions of Kv1.2 dynamics under physiological voltage changes. *Mol. Membr. Biol. 26*, 397−421.
(73) Treptow, W., Maigret, B., Chipot, C., and Tarek, M. (2004) Coupled motions between pore and voltage-sensor domains: A model for Shaker B, a voltage-gated potassium channel. *Biophys. J. 87*, 2365−2379.

(74) Tarek, M. (2005) Membrane Electroporation: A Molecular Dynamics Simulation. *Biophys. J. 88*, 4045−4053.
(75) Gumbart, J., Khalili-Araghi, F., Sotomayor, M., and Roux, B. (2012) Constant electric field simulations of the membrane potential illustrated with simple systems. *Biochim. Biophys. Acta 1818*, 294−302.
(76) Sachs, J. N., Crozier, P. S., and Woolf, T. B. (2004) Atomistic simulations of biologically realistic transmembrane potential gradients. *J. Chem. Phys. B 121*, 10847−10851.
(77) Delemotte, L., Dehez, F., Treptow, W., and Tarek, M. (2008) Modeling membranes under a transmembrane potential. *J. Chem. Phys. B 112*, 5547−5550.
(78) Fedida, D., and Hesketh, J. C. (2001) Gating of voltage-dependent potassium channels. *Prog. Biophys. Mol. Biol. 75*, 165−199.
(79) Zagotta, W. N., Hoshi, T., and Aldrich, R. W. (1994) Shaker potassium channel gating. III: Evaluation of kinetic models for activation. *J. Gen. Physiol. 103*, 3121−362.
(80) Schoppa, N. E., and Sigworth, F. J. (1998) Activation of Shaker potassium channels. III. An activation gating model for wild-type and V2 mutant channel. *J. Gen. Physiol. 111*, 313−342.
(81) Loboda, A., and Armstrong, C. M. (2001) Resolving the gating charge movement associated with late transitions in K channel activation. *Biophys. J. 81*, 905−916.
(82) Sigg, D., Bezanilla, F., and Stefani, E. (2003) Fast gating in the Shaker K^+ channel and the energy landscape of activation. *Proc. Natl. Acad. Sci. U.S.A. 100*, 7611−7615.
(83) Lin, M. A., Hsieh, J.-Y., Mock, A. F., and Papazian, D. M. (2011) R1 in the Shaker S4 occupies the gating charge transfer center in the resting state. *J. Gen. Physiol. 138*, 155−163.
(84) Vargas, E., Bezanilla, F., and Roux, B. (2011) In search of a consensus model of the resting state of a voltage-sensing domain. *Neuron 72*, 713−720.
(85) Roux, B. (2008) The membrane potential and its representation by a constant electric field in computer simulations. *Biophys. J. 95*, 4205−4216.
(86) Stefani, E., Toro, L., Perozo, E., and Bezanilla, F. (1994) Gating of Shaker K^+ channels: I. Ionic and gating currents. *Biophys. J. 66*, 996−1010.
(87) Lecar, H., Larsson, H. P., and Grabe, M. (2003) Electrostatic model of S4 motion in voltage-gated ion channels. *Biophys. J. 85*, 2854−2864.
(88) Grabe, M., Lecar, H., Jan, Y. N., and Jan, L. Y. (2004) A quantitativement assessment of models for voltage-dependent gating ion channels. *Proc. Natl. Acad. Sci. U.S.A. 101*, 17640−17645.
(89) Nonner, W., Peyser, A., Gilespie, D., and Eisenberg, B. (2004) Relating microscopic charge movement to macroscopic currents: The Ramo-Schockley Theorem applied to ion channels. *Biophys. J. 87*, 3716−3722.
(90) Papazian, D. M., Timpe, L. C., Jan, Y. N., and Jan, L. Y. (1991) Alteration of voltage-dependance of Shaker potassium channel by mutations in the S4 sequence. *Nature 349*, 305−310.
(91) Baker, O. S., Larsson, H. P., Mannuzzu, L. M., and Isacсoff, E. Y. (1998) Three transmembrane conformations and sequence-dependent displacement of S4 domain in K channels gating. *Neuron 20*, 1283−1294.
(92) Tiwari-Woodruff, S. K., Lin, M. A., Schulteis, C. T., and Papazian, D. M. (2000) Voltage-dependent structural interactions in the Shaker K^+ channel. *J. Gen. Physiol. 115*, 123−138.
(93) Planells-Cases, R., Ferrer-Montiel, A. V., Patten, C. D., and Montal, M. (1995) Mutation of conserved negatively charged residues in the S2 and S3 transmembrane segments of a mammalian K^+ channel selectively modulates channel gating. *Proc. Natl. Acad. Sci. U.S.A. 92*, 9422−9426.
(94) Vargas, E., Yarov-Yarovoy, V., Khalili-Araghi, F., Catterall, W. A., Klein, M. L., Tarek, M., Lindahl, E., Schulten, K., Perozo, E., Bezanilla, F., and Roux, B. (2012) An emerging consensus on voltage-dependent gating from computational modeling and molecular dynamics simulations. *J. Gen. Physiol. 140*, 587−594.
(95) Chipot, C., and Pohorille, A., Eds. (2007) *Free Energy Calculations: Theory and Applications in Chemistry and Biology*, Springer, Berlin.
(96) Pohorille, A., Jarzynski, C., and Chipot, C. (2010) Good practices in free-energy calculations. *J. Phys. Chem. B 114*, 10235−10253.
(97) Beckstein, O., Tai, K., and Sansom, M. S. (2004) Not ions alone: Barriers to ion permeation in nanopores and channels. *J. Am. Chem. Soc. 126*, 14694−14695.
(98) Darve, E., and Pohorille, A. (2001) Calculating free energies using average force. *J. Chem. Phys. 115*, 9169−9183.
(99) Hénin, J., and Chipot, C. (2004) Overcoming free energy barriers using unconstrained molecular dynamics simulations. *J. Chem. Phys. 121*, 2904−2914.
(100) Treptow, W., and Tarek, M. (2006) Molecular restraints in the permeation pathway of ion channels. *Biophys. J. 91*, L26−L28.
(101) Nury, H., Poitevin, F., Renterghem, C. V., Changeux, J. P., Corringer, P. J., Delarue, M., and Baaden, M. (2010) One-microsecond molecular dynamics simulation of channel gating in a nicotinic receptor homologue. *Proc. Natl. Acad. Sci. U.S.A. 107*, 6275−6280.
(102) Sotomayor, M., and Schulten, K. (2004) Molecular dynamics study of gating in the mechanosensitive channel of small conductance MscS. *Biophys. J. 87*, 3050−3065.
(103) Treptow, W., and Klein, M. L. (2010) The membrane-bound state of K2P potassium channels. *J. Am. Chem. Soc. 132*, 8145−8151.
(104) Barber, A. F., Carnevale, V., Raju, S. G., Amaral, C., Treptow, W., and Klein, M. L. (2012) Hinge-bending motions in the pore domain of a bacterial voltage-gated sodium channel. *Biochim. Biophys. Acta 1818*, 2120−2125.
(105) Jensen, M. U., Borhani, D. W., Lindorff-Larsen, K., Maragakis, P., Jogini, V., Eastwood, M. P., Dror, R. O., and Shaw, D. E. (2010) Principles of conduction and hydrophobic gating in K^+ channels. *Proc. Natl. Acad. Sci. U.S.A. 107*, 5833−5838.
(106) Beckstein, O., and Sansom, M. S. P. (2004) The influence of geometry, surface character, and flexibility on the permeation of ions and water through biological pores. *Phys. Biol. 1*, 42−52.
(107) Yifrach, O., and MacKinnon, R. (2002) Energetics of Pore Opening in a Voltage-Gated K^+ Channel. *Cell 111*, 231−239.
(108) Lu, Z., Klem, A. M., and Ramu, Y. (2002) Coupling between voltage sensors and activation gate in voltage-gated K^+ channels. *J. Gen. Physiol. 120*, 663−676.
(109) Van Slyke, A. C., Rezazadeh, S., Snopkowski, M., Shi, P., Allard, C. R., and Claydon, T. W. (2010) Mutations within the S4-S5 linker alter voltage sensor constraints in hERG K^+ channels. *Biophys. J. 99*, 2841−2852.
(110) Haddad, G. A., and Blunck, R. (2011) Mode shift of the voltage sensors in Shaker K^+ channels is caused by energetic coupling to the pore domain. *J. Gen. Physiol. 137*, 455−472.
(111) Meisel, E., Dvir, M., Haitin, Y., Giladi, M., Peretz, A., and Attali, B. (2012) KCNQ1 channels do not undergo concerted but sequential gating transitions in both the absence and the presence of KCNE1 protein. *J. Biol. Chem. 287*, 34212−34224.
(112) Kwan, D. C. H., Prole, D. L., and Yellen, G. (2012) Structural changes during HCN channel gating defined by high affinity metal bridges. *J. Gen. Physiol. 140*, 279−291.
(113) Chakrapani, S., Sompornpisut, P., Intharathep, P., Roux, B., and Perozo, E. (2010) The activated state of a sodium channel voltage sensor in a membrane environment. *Proc. Natl. Acad. Sci. U.S.A. 107*, 5435−5440.
(114) Amaral, C., Carnevale, V., Klein, M. L., and Treptow, W. (2012) Exploring conformational states of the bacterial voltage-gated sodium channel NavAb via molecular dynamics simulations. *Proc. Natl. Acad. Sci. U.S.A. 109*, 21336−21341.
(115) Schlitter, J., Engels, M., and Krüger, P. (1994) Targeted molecular dynamics: A new approach for searching pathways of conformational transitions. *J. Mol. Graphics 12*, 84−89.

(116) Barber, A. F., Liang, Q., Amaral, C., Treptow, W., and Covarrubias, M. (2011) Molecular mapping of general anesthetic sites in a voltage-gated ion channel. *Biophys. J. 101*, 1613−1622.
(117) Gosselin-Badaroudine, P., Delemotte, L., Moreau, A., Klein, M. L., and Chahine, M. (2012) Gating pore currents and the resting state of Nav1.4 voltage sensor domains. *Proc. Natl. Acad. Sci. U.S.A. 109*, 19250−19255.
(118) Zhou, M., Morais-Cabral, J. H., Mann, S., and MacKinnon, R. (2001) Potassium channel receptor site for the inactivation gate and quaternary amine inhibitors. *Nature 411*, 657−661.
(119) Domene, C., Klein, M. L., Branduardi, D., Gervasio, F. L., and Parrinello, M. (2008) Conformational Changes and Gating at the Selectivity Filter of Potassium Channels. *J. Am. Chem. Soc. 130*, 9474−9480.
(120) Cuello, L. G., Jogini, V., Cortes, D. M., and Perozo, E. (2010) Structural mechanism of C-type inactivation in K^+ channels. *Nature 466*, 203−208.
(121) Catterall, W. A. (2000) From ionic currents to molecular mechanisms: The structure and function of voltage-gated sodium channels. *Neuron 26*, 13−25.
(122) Yue, L., Navarro, B., Ren, D., Ramos, A., and Clapham, D. E. (2002) The cation selectivity filter of the bacterial sodium channel, NaChBac. *J. Gen. Physiol. 120*, 845−853.
(123) Zhao, Y., Yarov-Yarovoy, V., Scheuer, T., and Catterall, W. A. (2004) A gating hinge in Na^+ channels; a molecular switch for electrical signaling. *Neuron 41*, 859−865.
(124) Zhao, Y., Scheuer, T., and Catterall, W. A. (2004) Reversed voltage-dependent gating of a bacterial sodium channel with proline substitutions in the S6 transmembrane segment. *Proc. Natl. Acad. Sci. U.S.A. 101*, 17873−17878.
(125) Pavlov, E., Bladen, C., Winkfein, R., Diao, C., Dhaliwal, P., and French, R. J. (2005) The pore, not cytoplasmic domains, underlies inactivation in a prokaryotic sodium channel. *Biophys. J. 89*, 232−242.
(126) Irie, K., Kitagawa, K., Nagura, H., Imai, T., Shimomura, T., and Fujiyoshi, Y. (2010) Comparative Study of the Gating Motif and C-type Inactivation in Prokaryotic Voltage-gated Sodium Channels. *J. Biol. Chem. 285*, 3685−3694.
(127) Eriksson, M. A. L., and Roux, B. (2002) Modeling the structure of Agitoxin in complex with the Shaker K^+ channel: A computational approach based on experimental distance restraints extracted from thermodynamic mutant cycles. *Biophys. J. 83*, 2595−2609.
(128) Wang, J., Yarov-Yarovoy, V., Kahn, R., Gordon, D., Gurevitz, M., Scheuer, T., and Catterall, W. A. (2011) Mapping the receptor site for α-scorpion toxins on a Na^+ channel voltage sensor. *Proc. Natl. Acad. Sci. U.S.A. 108*, 15426−15431.
(129) Ouyang, W., Jih, T. Y., Zhang, T. T., Correa, A. M., and Hemmings, H. C. J. (2007) Isoflurane inhibits NaChBac, a prokaryotic voltage-gated sodium channel. *J. Pharmacol. Exp. Ther. 322*, 1076−1083.
(130) Catterall, W. A., Cestèle, S., Yarov-Yarovoy, V., Yu, F. H., Konoki, K., and Scheuer, T. (2007) Voltage-gated ion channels and gating modifier toxins. *Toxicon 49*, 124−141.
(131) Delemotte, L., Treptow, W., Klein, M. L., and Tarek, M. (2010) Effect of sensor domain mutations on the properties of voltage-gated ion channels: Molecular dynamics studies of the potassium channel Kv1.2. *Biophys. J. 99*, L72−L74.
(132) Khalili-Araghi, F., Tajkhorshid, E., Roux, B., and Schulten, K. (2012) Molecular Dynamics Investigation of the ω-Current in the Kv1.2 Voltage Sensor Domains. *Biophys. J. 102*, 258−267.
(133) Tombola, F., Pathak, M. M., and Isacoff, E. Y. (2005) Voltage-sensing arginines in a potassium channel permeate and occlude cation-selective pores. *Neuron 45*, 379−388.
(134) Tombola, F., Pathak, M. M., Gorostiza, P., and Isacoff, E. Y. (2007) The twisted ion-permeation pathway of a resting voltage-sensing domain. *Nature 445*, 546−549.